Title

Mechanism and Dynamics of Molecular Exchange at the Silica/Binary Solvent Mixtures Interface

Journal

The Journal of Physical Chemistry A, 119(50)

ISSN

1089-5639

Authors

Karnes, John J
Benjamin, Ilan

Publication Date

2015-12-17

DOI

10.1021/acs.jpca.5b05097

Peer reviewed

Mechanism and dynamics of molecular exchange at the silica/binary solvent mixtures interface

*John J. Karnes and Ilan Benjamin**

Department of Chemistry and Biochemistry

University of California Santa Cruz, CA 95064

Abstract:

Non-equilibrium molecular dynamics simulations of acetonitrile/methanol mixtures in contact with a hydroxylated silica surface are used to elucidate the mechanism of molecular exchange at a hydrophilic liquid/solid interface. The different hydrogen-bonding ability of the two solvents provides a driving force for the adsorption/desorption process, which is followed by examining several structural and energetic properties of the system. Two different reaction coordinates for the hydrogen bonding exchange are defined and are used to identify transition states in which the methanol attains a well-defined orientation. The reaction coordinates are used to examine the mechanism and dynamics of the exchange. We find that the exchange process involves multiple recrossing of the transition state and can progress via two different mechanisms, depending whether the methanol first acts as a hydrogen bond donor or acceptor at the silica surface.

*Email: benjamin@chemistry.ucsc.edu , Telephone: 831-459-3152

I. Introduction

Molecular structure and dynamics at interfaces dictate behavior in many processes of interest. The silica surface is particularly of interest to researchers due to its abundance in nature and general utility. The need for molecular insight into behavior at this surface inspires current work in several disparate fields, including the frontiers of drug delivery,[1-4] geology,[5, 6] catalysis,[7] high performance liquid chromatography,[8-12] and astrophysics.[13-15] Silica is also an excellent model hydrophilic surface for work that specifically focuses on the solid-liquid interface.

Experimental difficulty arises due to the buried nature of the solid-liquid interface, but advances in nonlinear spectroscopy, particularly vibrational sum frequency generation spectroscopy,[16, 17] have resulted in a continued increase in understanding the silica-liquid interface, with significant work devoted to water,[18-20] alcohol,[16, 21-23] and alkyl cyanide[24, 25] liquid phases. Molecular dynamics simulations of these systems[22, 26-32] provide molecularly detailed insight into the system and have been used extensively in conjunction with nonlinear optical experiments to fully elucidate interfacial organization and orientation.

Behavior at the silica-liquid interface varies depending on the nature of the liquid. For example, the polar aprotic acetonitrile exhibits antiparallel dipole-dipole pairing in bulk liquid. At a hydroxylated silica surface, acetonitrile molecules are able to accept hydrogen bonds from the silica surface silanol groups, interactions significantly stronger than dipole pairing. This hydrogen bonding causes the interfacial acetonitrile to align approximately perpendicular to the interface. Interstitial acetonitrile molecules then align themselves into a dipole-paired sublayer nearly antiparallel to the interfacial acetonitrile.[31] Saturated straight-chain alcohols have different

hydrogen bonding behavior: they may act as both hydrogen bond donors and acceptors. At a solid silica surface the alcohols' hydroxyl groups hydrogen bond with the silica surface and their alkane tails align to create a surface-induced hydrophobic region that prohibits neighboring alcohol solvent layers from interacting with the surface.[23]

Recent work has investigated binary solvents as silica's adjacent liquid phase.[11, 33-35] This next level of complexity requires the understanding of both solvent-solvent interactions and allows researchers to observe the interplay between dissimilar solid-liquid interactions in a situation where active sites at the solid surface are a limited resource. It is well established that interfacial behavior differs from bulk and in the case of binary solvents interfacial mole fractions often differ significantly from the bulk. For example, Melnikov et. al report that a liquid methanol-acetonitrile mixture with a 2/98 (v/v) bulk ratio at a silica interface has over 50% of the silica surface OH groups bonded to methanol molecules.[11] Bulk-interface inhomogeneity in binary solvent systems may be used to enhance separation processes and are inherent in gradient elution, but the same mechanism may also amplify interface contamination in systems.

In the present work we focus on gaining molecular insight into the dynamics and mechanism by which a hydrophilic solid surface segregates a binary solvent mixture. Specifically, we consider the molecularly detailed events associated with the solvent exchange at the interface between methanol/acetonitrile mixtures and a hydroxylated silica surface. This system behaves similarly to a standard configuration of hydrophilic interaction liquid chromatography (HILIC).[10, 36] HILIC is a liquid chromatographic technique that incorporates hydrophilic stationary and mobile phases, the most common mobile phase consisting of an acetonitrile-water mixture. The mobile phase typically has a low (<3%) mole fraction of water. Since water preferentially organizes at the hydrophilic surface of the stationary phase, the

resulting inhomogeneous binary solvent performs a pseudo liquid-liquid extraction and is able to separate polar analytes where more conventional liquid chromatography fails. Recent simulation work has investigated the segregation of solvents in model HILIC systems and supported the theory of a water-rich, mostly immobile solvent layer at the solid-liquid interface that extends 1.5 nm from the silica surface and reduces translational mobility of polar analytes.[12]

In this paper, using non-equilibrium molecular dynamics simulations, we examine the energetic and structural characteristics of the silica-methanol-acetonitrile system as it approaches equilibrium and quantify the dynamics associated with the single molecular exchange event at the interface. This provides us with a molecularly detailed mechanism by which hydrogen bonding molecules undergo exchange at a hydrophilic liquid/solid interface.

The rest of the paper is organized as follows. In section II we briefly describe the system structure and potential energy used. In section III we describe and discuss of the results of several types of molecular dynamics simulations. Conclusions are presented in section IV.

II. Systems and Methods

Molecular dynamics simulations are performed utilizing a "box" with dimensions L_x = 45.0 Å, L_y = 43.3 Å, and L_z = 100 Å. The box contains a silica surface in the *x*-*y* plane in contact with a total of 1023 solvent molecules, with varying compositions as described below, with periodic boundary conditions extending in the *x* and *y* directions. The geometry of the silica surface is based on the work of Lee and Rossky[28] and consists of a fully-hydroxylated β-Cristobalite surface. Our surface differs by incorporating terminal silanol groups with fully flexible bonds at the silica surface, using the CHARMM water contact angle Lennard-Jones and bond parameters.[37, 38] Each silica surface consists of 90 silanol sites: a density of 4.62 /nm^2. The

acetonitrile and methanol force field parameters are those used in our earlier work[39, 40] that employ a united atom, three-site description of each solvent. Intermolecular potentials are calculated as the sum of Lennard-Jones and Coulomb terms:

$$u_{ij}(r) = 4\varepsilon_{ij}\left[\left(\frac{\sigma_{ij}}{r}\right)^{12} - \left(\frac{\sigma_{ij}}{r}\right)^{6}\right] + \frac{q_i q_j}{4\pi r \varepsilon_0} \quad (1)$$

where *i* and *j* denote atoms on different molecules separated by a distance *r*. Mixed Lennard-Jones interactions between all species are calculated using Lorentz-Berthelot combining rules: $\sigma_{ij} = (\sigma_i + \sigma_j)/2$ and $\varepsilon_{ij} = (\varepsilon_i \varepsilon_j)^{1/2}$. All simulations are performed using our in-house MD code that incorporates the velocity form of the Verlet algorithm and used an integration time step of 0.5 fs.

A key ingredient in characterizing the system is a definition of the solvent-silica hydrogen bonding. We use geometrical definitions of silica-methanol[22] and acetonitrile-silica[41] hydrogen bonds where a bond is considered present if the H-O-acceptor angle is less than 30º and the donor oxygen-acceptor distance is less than 3.4 Å for silica-methanol bonds and less than 3.5 Å for silica-acetonitrile bonds.

We perform the following simulations:

1. 16.5 ns simulations starting from 20 independent configurations of randomly prepared mixtures with several different acetonitrile mole fractions in contact with a silica surface. These calculations provide an overall global tracking of the adsorption/desorption process.

2. 1300 trajectories starting from independent configurations where a single methanol is dissolved in acetonitrile near the surface. These simulations provide the single molecule equivalent of the trajectories in part 1 above and are used to collect the initial conditions for extensive "reactive" trajectories by saving system configurations when methanol-silica hydrogen bonds are first detected.
3. These configurations are used to obtain thousands of "reactive" trajectories where the methanol molecule displaces an adsorbed acetonitrile molecule. This is done for the mechanistic studies and for the computation of reactive flux correlation functions (described below).

Additional details on the calculations performed are given below.

III. Results and discussion

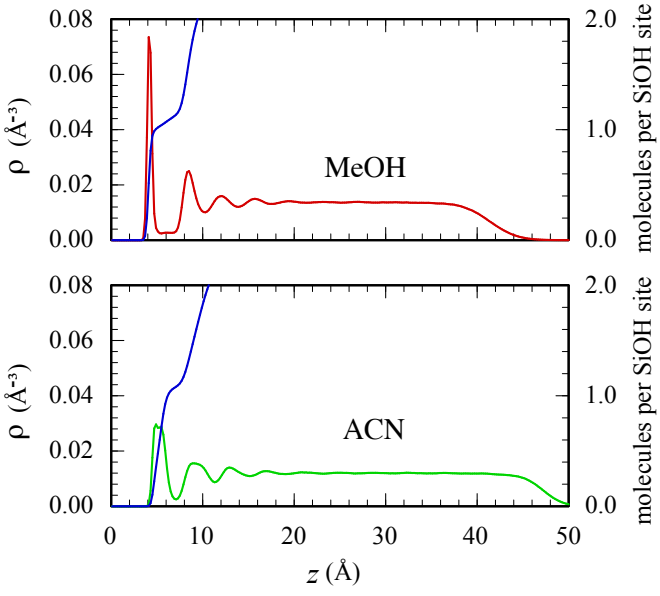

Figure 1. Density profiles of neat methanol (top, red) and neat acetonitrile (bottom, green) at the liquid-silica interface. The blue line in each panel represents the cumulative number of liquid molecules per silica site (right axis).

As a reference for our mixture calculations, in Figure 1 we show the center-of-mass density profiles of the two neat liquids in contact with the silica surface. These density profiles illustrate the liquids' different behavior at the hydrophilic silica interface. Methanol is able to hydrogen bond with surface silica sites as both donor and acceptor to form a densely packed, highly ordered monolayer at the solid-liquid interface, seen as the first sharp peak in the density profile and correspond to approximately one methanol molecule per silica site. This surface hydrogen bonding induces order in the methanol methyl groups, forming a hydrophobic region that excludes other polar methanol molecules, resulting in the low-density region between the first and second density peaks. Acetonitrile is also polar but only able to act as a hydrogen bond acceptor. The silica surface induces order by hydrogen bonding with acetonitrile but allows sufficient spacing for a second sublayer of acetonitrile molecules to align themselves interstitially and antiparallel to the hydrogen bonded acetonitrile. This is seen in the much wider first peak (compared with methanol). However, it still corresponds to a full monolayer coverage (note the kink in the blue line). Dipole-dipole pairing is seen in bulk acetonitrile, but surface-induced order leads to formation of a bilayer-like structure at the solid-liquid interface. Beyond the first solvent layer the density profiles of both neat liquids oscillate for several periods before reaching bulk behavior at $z \approx 25$ Å. For future reference, we define the "bulk region" to be the region 25 Å $< z <$ 34 Å.

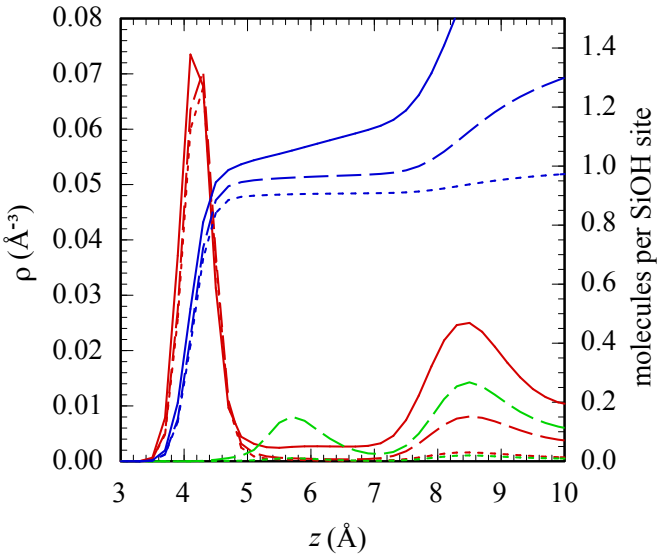

Figure 2. Density profiles of methanol (red lines) and acetonitrile (green lines) in several binary acetonitrile-methanol mixtures in contact with a silica surface. The blue lines represent the cumulative number of methanol molecules per silica site (right axis). Shown are representative systems of neat methanol (solid curves) and mixtures in which the acetonitrile bulk mole fractions are $x_{ACN,bulk} = 0.64$ (dashed curves), and $x_{ACN,bulk} = 0.94$ (dotted curves).

Consider next the density profiles of the two liquids in a binary mixture at the silica surface, as shown in Figure 2. These density profiles highlight methanol's affinity for the surface. The first solvent peak, representing methanol molecules hydrogen-bonded to the silica surface is only weakly dependent on the equilibrium bulk mole fraction of acetonitrile as it increases from 0 to 0.94. As the acetonitrile concentration increases, the first acetonitrile density peak, centered at 5.6 Å, appears. This peak consists of acetonitrile molecules that orient their dipoles antiparallel to the methanol O-CH_3 vectors, exhibiting the same behavior as molecules in the second sublayer of the neat acetonitrile-silica system. Integrated methanol densities, shown in Figure 2 as molecules per silica site, highlight the difference in methanol surface coverage. These values

remain quite similar through the first solvent layer before diverging dramatically due to the large differences in mole fraction beyond the hydrogen bonded interfacial layer.

To study the non-equilibrium solvent exchange dynamics at the surface, mixtures of methanol-acetonitrile are prepared by either replacing randomly selected acetonitrile molecules by methanol molecules starting from neat acetonitrile or conversely by starting from a neat methanol system and replacing a number of randomly selected methanol molecules by acetonitrile. 20 independent initial configurations are used. After a short equilibration process to remove high-energy configurations, the binary systems are further allowed to relax to the final equilibrium state. During this process, methanol molecules gradually displace acetonitrile molecules adsorbed at the silica surface. Figure 3 summarizes the dynamics as the system approaches equilibrium.

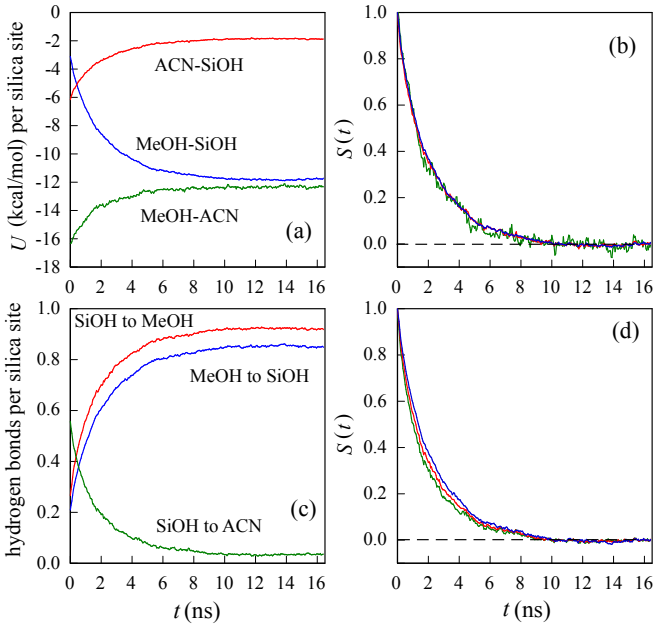

Figure 3. Time-dependent relaxation toward equilibrium of a methanol-acetonitrile mixture ($x_{ACN} = 0.94$) at a silica surface starting from a random molecular composition. (a) Silica-solvent

and solvent-solvent interaction energies and (b) the corresponding normalized non-equilibrium correlation function (see Eq. 2 for a definition). (c) Silica-solvent hydrogen bonding probability and (d) the corresponding normalized non-equilibrium correlation function.

System interaction energies are depicted in Figure 3a. As the relaxation proceeds, methanol-silica interaction energy increases (becomes more negative) as methanol molecules move to the interface. As acetonitrile molecules are displaced from the surface, their interaction with the silica surface and with the significant number of methanol molecules migrating to the surface decreases. Relaxation of the interaction energy to its equilibrium value occurs in approximately 12 ns for a system with a bulk acetonitrile mole fraction of 0.94. Silica-solvent hydrogen bonding during these relaxations is shown in Figure 3c. As methanol molecules populate the surface, silica sites are able to participate in hydrogen bonds as donor and acceptor, a more energetically favorable configuration than an interface dominated by acetonitrile molecules, which can only accept hydrogen bonds from the silica surface.

This binary mixture demonstrates the affinity of the silica surface for methanol over acetonitrile. In this representative binary mixture, with a bulk methanol mole fraction of 0.06, 92% of the silica sites donate hydrogen bonds to methanol molecules (red line in Figure 3c) and 85% of these sites accept hydrogen bonds from these same methanol molecules (blue line in Figure 3c). A given silanol site has only a 3% likelihood of participating in a hydrogen bond with an acetonitrile molecule. Silica-methanol interaction energy at equilibrium is approximately 6 times greater than silica-acetonitrile.

To gain additional insight into the relaxation progress independent of the property examined, Figures 3b and 3d show the corresponding normalized non-equilibrium correlation functions, which are defined as:

$$S(t) = \frac{\overline{\Gamma}(t) - \overline{\Gamma}(\infty)}{\overline{\Gamma}(0) - \overline{\Gamma}(\infty)} \tag{2}$$

for any property of interest Γ, where $\overline{\Gamma}(t)$ is the average at time t over all initial configurations. The interaction energies and hydrogen bonding probabilities show very similar time-dependent behavior. It is nearly exponential with a time constant of 2.3 ns. This behavior suggests that the underlying molecular events governing the relaxation are independent replacements of an adsorbed acetonitrile molecule by a methanol molecule, so that the formation of silica-methanol hydrogen bonds is accompanied by the breaking of a silica-acetonitrile hydrogen bond. Acetonitrile molecules subsequently migrate away from the silica surface.

It is interesting to compare the non-equilibrium relaxation described above with the relaxation of the fluctuations at equilibrium. To do this, we consider the final 4.5 ns of the trajectories of Figure 3 as representative of the system at equilibrium. To avoid confusion between equilibrium and non-equilibrium calculations, we define Γ_e to be the property of interest during the equilibrium portion of the trajectories that correspond to Γ. With these definitions, we may compare the fluctuations of the interaction energies and hydrogen bonding probabilities during this equilibrium period. As a rough measure for the size of the equilibrium fluctuations, we consider the ratio of the standard deviation at equilibrium: $\sigma = \left\langle (\delta\Gamma_e)^2 \right\rangle^{1/2} = \left\langle \left(\Gamma_e(t) - \left\langle \Gamma_e \right\rangle \right)^2 \right\rangle^{1/2}$ to the total non-equilibrium change $\overline{\Gamma}(0) - \overline{\Gamma}(\infty)$. (Note that $\overline{\Gamma}(\infty) = \left\langle \Gamma_e \right\rangle$). This ratio is equal to $0.04 - 0.05$ for the hydrogen bonding probabilities and for the solvent-silica interaction energies but considerably greater (0.12) for the methanol-acetonitrile interaction energy. The methanol-acetonitrile interaction energy is the only parameter not a strong function of the hydrogen bonding at the silica surface,

so these results suggest much stronger constraint on the size of the fluctuations associated with the surface hydrogen bonding.

It is also interesting to contrast the non-equilibrium correlation functions $S(t)$ of Eq. 2 (shown on the right panels of Figure 3) with the equilibrium correlation functions defined as

$$C(t) = \frac{\langle \delta\Gamma_e(t)\delta\Gamma_e(0)\rangle}{\langle \delta\Gamma_e(0)\delta\Gamma_e(0)\rangle} \tag{3}$$

These correlations functions are shown in Figure 4 together with the exponential fit to the non-equilibrium correlation functions (fit to the average of all six $S(t)$ curves, which essentially fall on top of each other).

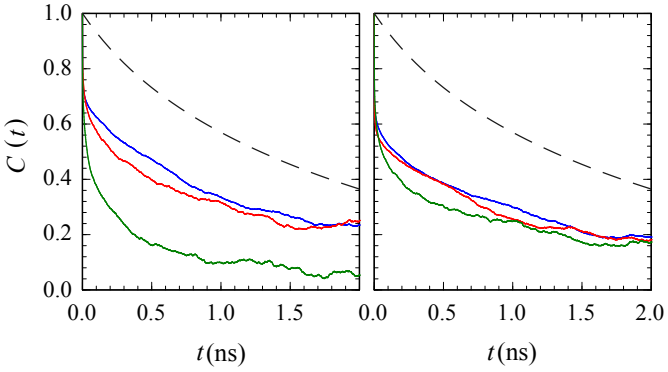

Figure 4. Left: Normalized equilibrium correlation functions (Eq. 3) of methanol-silica, acetonitrile-silica, and methanol-acetonitrile interaction energies (blue, red, and green lines, respectively). Right: Silica to methanol, methanol to silica, and silica to acetonitrile hydrogen bonding probability equilibrium correlation functions (blue, red, and green lines, respectively) Dashed lines show the non-equilibrium relaxations.

Figure 4 emphasizes the considerably different time scales for the non-equilibrium vs. equilibrium decay. The later is much faster since it is dominated by the fluctuations of an already

existing hydrogen bond, while the non-equilibrium relaxation is dominated by adsorption/desorption events. The fastest equilibrium decay is observed in the interaction energy of the two-solvents; a relaxation essentially independent of the surface dynamics.

To gain detailed molecular level understanding of the mechanism and dynamics underlying the process by which a methanol molecule displaces an acetonitrile molecule at the silica surface, we next study a model system of neat acetonitrile at a silica surface where one random acetonitrile molecule in the second solvent layer (8.5 Å < z < 10.5 Å) is replaced by methanol. A harmonic reflecting potential affecting only the methanol is placed at z = 11 Å to prevent this molecule from diffusing into the bulk acetonitrile. After a short equilibration process where the methanol reaches an equilibrium with the surrounding acetonitrile molecules, the configuration is saved and the process is repeated to generate 10 independent configurations. 130 trajectories are generated from each configuration by assigning random velocities to all atoms at time zero. The dynamics for these 1300 trajectories is quantified by detecting methanol-silica hydrogen bonding using the geometrical considerations described above. Since methanol can participate in two hydrogen bonds with the silica site, three possible methanol-silica hydrogen-bonding states are considered: methanol as donor, methanol as acceptor, or methanol participating in two hydrogen bonds with the surface as both donor and acceptor (denoted by k = d, a, or b, respectively). Each bonding parameter h_k is assigned a value of 0 if the bond of type k does not exist and 1 if the bond is present. With these definitions we may quantify the "reaction" progress as the probability that methanol-silica hydrogen bonding activity is detected:

$$P_k(t) = \frac{1}{N}\sum_{i}^{N} h_k(t) \tag{4}$$

where N is the number of trajectories. In computing $P_k(t)$, we use Absorbing Boundary Conditions (ABC), where, after an initial methanol-silica hydrogen bond is detected (either donor or acceptor), the trajectory is terminated if subsequently either no methanol-silica hydrogen bonds are detected for a duration of 2.0 ps ("reactant" side) or if the methanol acts as both donor and acceptor in two distinct methanol-silica hydrogen bonds for 2.0 ps ("product" side). (The 2 ps value is later justified by examining the recrossing dynamics at the "transition state".)

Figure 5 summarizes the early 70 ps of "reaction" progress, where approximately 17% of the trajectories resulted in methanol being bonded to the silica surface. The progress of the three discrete bonding states track closely together and steadily increase. Silica-methanol interaction energy (values depicted on the right axis), shown as the black curve in Figure 5, also tracks well with the reaction progress.

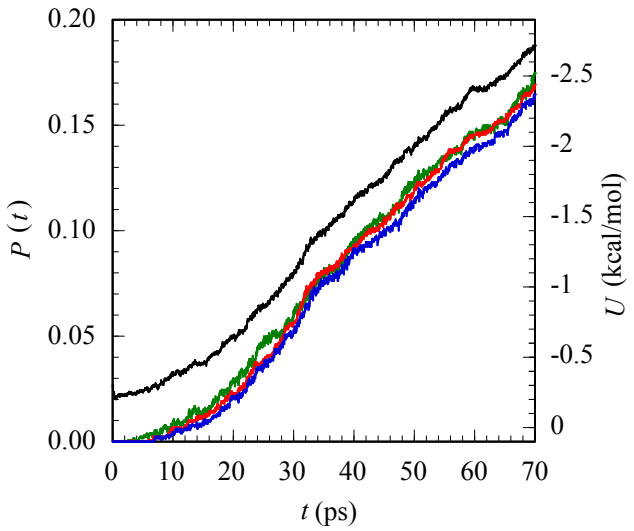

Figure 5. Reaction progress of a single methanol molecule adjacent to an acetonitrile-silica interface. Curves represent the probability of methanol hydrogen bonding with the silica surface where methanol acts as donor (blue), acceptor (red), or both donor and acceptor (green). Methanol-silica interaction energy (black) is shown on the right axis.

The dynamics described in Figure 5 include the "uninteresting" effect of the diffusion of the methanol molecule to the surface and as a result the wide distribution of arrival times at the surface. To disentangle this part from the actual solvent exchange process, MD trajectories were run starting from configurations obtained from the "reactive" events shown in Figure 5. These starting configurations are simulation snapshots collected at the time step when methanol-silica hydrogen bonds were first detected. A total of 120 different configurations, 40 corresponding to each different initial hydrogen bonding state $k = d$, a, or b, were generated for this set of simulations. 100 trajectories from each starting configuration were performed with initial random velocities assigned from a Maxwell-Boltzmann distribution and subject to the absorbing boundary conditions described earlier. The results are shown in Figure 6. All the curves start at $P_k = 1$ at $t = 0$ and immediately experience a sudden drop since the assignment of random velocities at the initial configuration typically results in the breakup of the bond (see below).

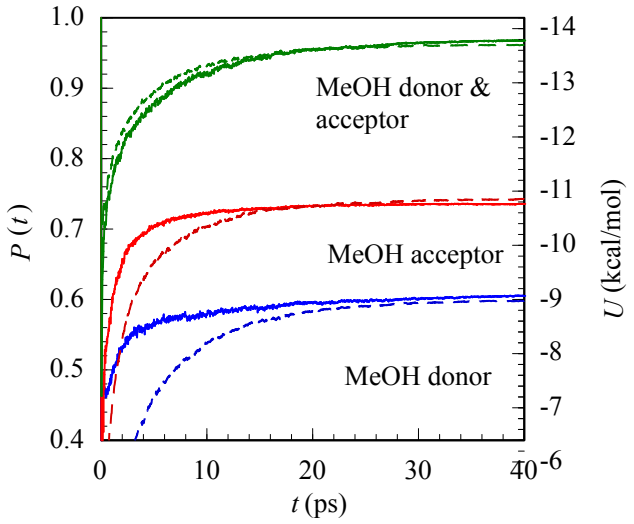

Figure 6. Reaction progress when methanol-silica hydrogen bonding is present at $t = 0$. Associated methanol-silica interaction energies (dashed curves) are shown on the right axis.

In the three starting configurations considered, the probability that the methanol molecule forms stable hydrogen bonds with the silica surface reaches a plateau at about 25 ps. This behavior can be compared to the reaction progress in Figure 5 where the probability of stable hydrogen bond formation reached only 0.17 and continues to linearly increase 70 ps into the simulations (due to the wide distribution of the methanol arrival times at the surface). It's important to keep in mind that the dynamics of hydrogen bond formation described in Figure 6 conservatively estimate the bonding progress from first bond detection since the randomized velocities allow for immediate dissociation of the bonds. For example, at the first time step of hydrogen bond detection, the O-O distance may be at the upper limit of the methanol-silica hydrogen bonding definition of 3.4 Å. If these oxygen molecules are assigned velocities in opposing directions, the bond will immediately be broken. The fact that the plateau value in Figure 6 is less than 1 is due to the subset of trajectories that did not maintain their hydrogen bonding state and were terminated by the

"reactants" ABC. Thus the utility of this plot is in demonstrating the different relative persistence of the three hydrogen bonding states.

When methanol first interacts with the silica surface as donor, the system is less likely to proceed to the product side than if the methanol first interacts as hydrogen bond acceptor (compare the plateau values of P(t) = 0.7 and P(t) = 0.6 for acceptor and donor initial states, respectively). This is likely due to the relative immobility and location of the silica oxygen atom relative to the other hydrogen bonding atoms. The methanol hydrogen-silica oxygen bond is less likely to survive because the silica oxygen is bonded to an immobile silicon atom, resulting in a less flexible bond. This same relationship is seen in studies of the neat silica-methanol interface where methanol-silica hydrogen bond lifetimes are reportedly shorter when methanol acts as donor.[42] However, we also note that methanol is more likely to first hydrogen bond with the silica surface as donor (61%) than as an acceptor (39%) (data obtained from the trajectories used to generate Figure 5).

Figure 6 also depicts the average methanol silica interaction energies for the three types of trajectories. The average energies of the starting configurations are –3.6, –4.3, and –9.2 kcal/mol for methanol acting as donor, acceptor, and both donor and acceptor, while the average silica/methanol interaction energy in the "products" side is $\langle U_p \rangle$ = –14.2 kcal/mol. The average energy scales with $P_k(t)$ near the plateau region so that the interaction energy at the plateau region $\langle U_k(\infty) \rangle$ is approximately equal to the plateau value of $P_k(t)$ times $\langle U_p \rangle$. Thus, the approach to the plateau region may be interpreted as the progress from one weakly bound to two stable methanol-silica hydrogen bonds.

We now turn to a detailed examination of the exchange mechanism. To this end it is useful to define a "reaction coordinate" that tracks the progress from a methanol molecule far

from the surface ("reactants") to a state where this molecule is bonded to the silica surface ("products"). When methanol adsorbs to the silica surface, silica-methanol hydrogen bonds form. Since the silica site is unable to stably donate hydrogen bonds to both a methanol molecule and an acetonitrile molecule, the silica-acetonitrile hydrogen bonds typically break. The distances used to geometrically detect hydrogen bonding may also be used to generate reaction coordinates to monitor the progress of this reactive event. Since methanol forms two hydrogen bonds at the surface we may define two independent reaction coordinates, illustrated in Figure 7.

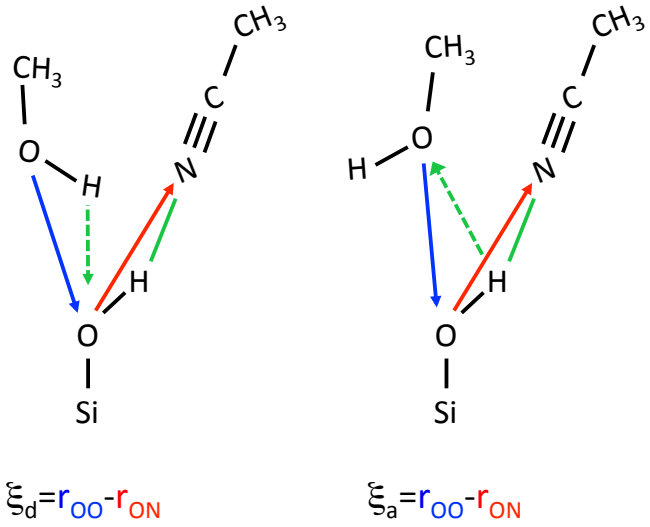

Figure 7. Reaction coordinates ξ_d (left) and ξ_a (right) representing methanol's hydrogen bonding relationship with a silica site as either donor or acceptor, respectively.

When methanol acts as a hydrogen bond donor, the reaction coordinate ξ_d is defined by locating the silica site whose oxygen atom is closest to the methanol hydrogen. The oxygen – oxygen distance between this silica site and the methanol oxygen is labeled r_{OO}. The distance between the silica oxygen and the nearest acetonitrile nitrogen atom is labeled r_{ON}. The collective

variable ξ_d is then defined as $\xi_d = r_{OO} - r_{ON}$. Similarly we define ξ_a to study the reactive event where the methanol molecule accepts a hydrogen bond from the silica surface. In this case, the relevant silica site is the site whose hydrogen atom is closest to the methanol oxygen atom (see right panel of Figure 7). The distances r_{OO} and r_{ON} are defined in the same manner as before; their difference is ξ_a. These definitions depend on identifying during the simulations the proper silica sites and we update these identities every 10 integration steps (5 fs of simulation time).

The values of the reaction coordinates ξ_d and ξ_a are calculated every 25 fs in simulations that resulted in a reactive event. We define this reactive event to be complete when the methanol molecule has been bonded to the silica surface by two hydrogen bonds for an uninterrupted period of 2.0 ps, identical to the product side ABC described above. Once the system reaches this state the trajectory is terminated. These distances are assembled into probability distributions in Figure 8. (The data used to generate these distributions are the subset of all the 1300 trajectories used to generate Figure 5 subject to the condition that the trajectory reached the "products" state and was terminated by the ABC).

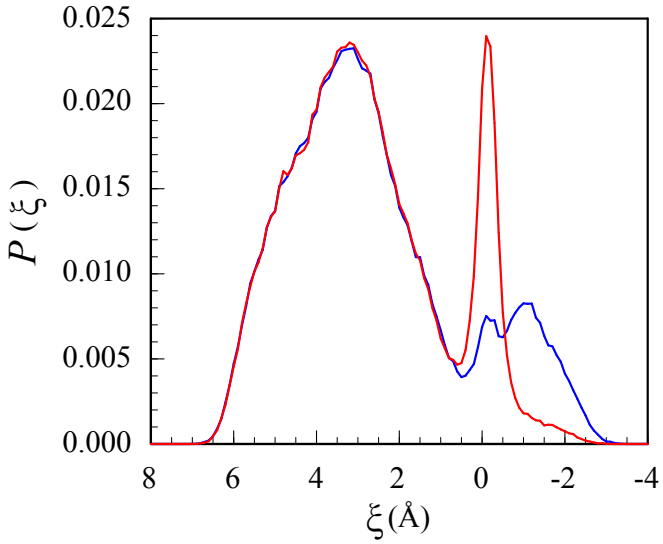

Figure 8. Probability distribution (normalized to unit area) of the reaction coordinates ξ_d (red curve) and ξ_a (blue curve).

The reaction progress can be followed from left to right on the ξ-axis, where positive values of ξ correspond to methanol far from the silica surface and negative values represent a state where the acetonitrile has desorbed. When methanol is far from the silica surface, the two curves corresponding to methanol acting as donor or acceptor are nearly identical because the r_{OO} distances (between the silica and methanol oxygens) dominate the values of both ξ_d and ξ_a. As the methanol-silica distance approaches the silica-acetonitrile distance, ξ_d and ξ_a both approach zero and the residence time of the system at these distances appears to decrease. We define these local minima as the transition states along these reaction coordinates at 0.5 Å and 0.6 Å for ξ_d and ξ_a, respectively.

The obvious differences between ξ_d and ξ_a are seen once the system is past the transition state and the methanol-silica hydrogen bonds form. When the methanol molecule acts as an acceptor and the silica site acts as donor (ξ_a), a small peak is present at $\xi_a = 0$, where the silica site can potentially serve as hydrogen bond donor to both methanol and the nearby acetonitrile. As the acetonitrile disassociates from the silica site and begins to diffuse away, ξ_a becomes more negative and peaks at −1 Å (representing the products state). In the histogram of this reaction coordinate, ξ_a, the dissociation of the acetonitrile from the silanol donor site is observed. When the silica site accepts a hydrogen bond from the methanol molecule (ξ_d), no competition for silica's role as donor to the nearby acetonitrile is introduced. The relevant silica site remains hydrogen bonded to an acetonitrile. Since the hydrogen bonds described by r_{OO} and r_{ON} may coexist and their equilibrium distances are similar, ξ_d exhibits a large sharp peak centered at 0 Å.

The overlaid histograms in Figure 8 also illustrate the mechanism by which methanol displaces acetonitrile from the silica surface: when a methanol molecule interacts with a silica site as hydrogen bond acceptor, the acetonitrile molecule bonded to the same site is displaced. The methanol molecule then hydrogen bonds to an adjacent silanol site as a hydrogen bond donor without affecting the silica-acetonitrile hydrogen bond.

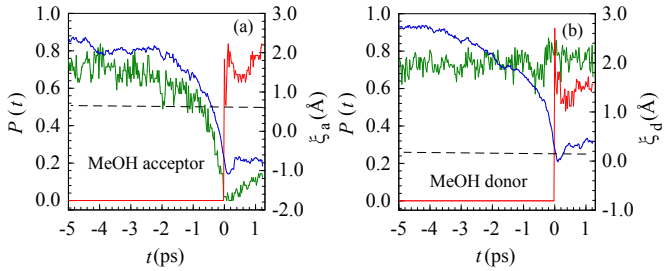

Figure 9. Hydrogen bond probabilities for silica-acetonitrile (green curves) and silica-methanol (red curves) when the methanol molecule engages the silica surface. The respective reaction coordinate (blue curves, right axes) are also displayed for events where methanol approaches a given silica site as acceptor (a) or donor (b). The black dotted lines represent the value of the reaction coordinate minima observed in Figure 8.

The specifics of this displacement are illustrated further in Figures 9a and 9b. In these plots, the reactive events described above have been time-shifted so that the initial silica-methanol hydrogen bond occurs at $t = 0$. In figure 9a (where methanol acts as an acceptor) the probability of a silica site donating a hydrogen bond to an acetonitrile molecule drops significantly before the silica-methanol hydrogen bond is initiated. In figure 9b (where the methanol acts as a donor) the situation is quite different. The silica-acetonitrile hydrogen bond exhibits no discernable awareness of the formation of a silica-methanol hydrogen bond when methanol acts as donor. The locations of the minima of the reaction coordinates ξ_a and ξ_d,

represented as the black dotted lines, add more mechanistic insight. In figure 9a, when methanol acts as hydrogen bond acceptor, the transition state ξ_a is crossed before formation of the silica-methanol hydrogen bond. In contrast, when methanol donates a hydrogen bond to silica, this hydrogen bond is detected at the same time the ξ_d transition state is crossed. This difference is further discussed below.

The above definitions of transition states based on these geometrical reaction coordinates ξ_d and ξ_a permit investigation of the methanol-silica reactive event. In particular, we consider the deviation from transition state theory, which states that after reaching the transition state the trajectory proceeds to the products side without any recrossing. Recrossings of the transition state may be attributed to solvent effects, here the neighboring acetonitrile molecules. To quantify the likelihood of these recrossings we calculated the reactive flux correlation functions for each of the reaction coordinates. In brief, molecular dynamics simulations are run starting with an initial configuration where the methanol molecule is at the transition state ξ_d or ξ_a. The MD trajectory begins with random velocities assigned from a flux-weighted Maxwell-Boltzmann distribution so that the value of $d\xi/dt$ is positive at $t = 0$. The normalized reactive flux correlation function for this system was calculated by:[43]

$$\kappa(t) = \frac{1}{N}\sum_{i=1}^{N} H\left[\xi_i(t) - \xi_i(0)\right] \tag{5}$$

where κ is transmission coefficient, ξ_i is the reaction coordinate value of the ith trajectory at time t, and H is the Heaviside function ($H(x) = 0$ for $x < 0$; $H(x) = 1$ for $x > 0$). These curves are shown in Figure 10.

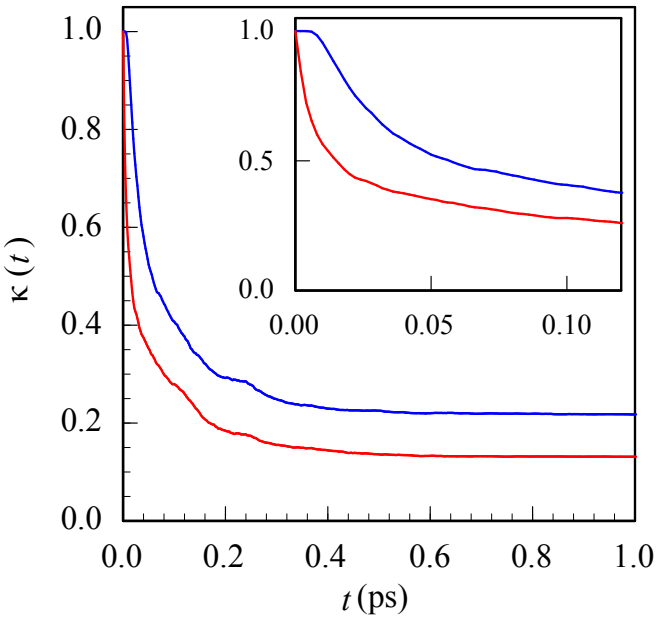

Figure 10. Reactive flux correlation functions for the reaction coordinates ξ_d (red curves) and ξ_a (blue curves).

The values of $\kappa(t)$ reach a plateau at ~600 fs. We assign the values of these plateaus as transmission coefficients of the respective reaction coordinates, $\kappa_a = 0.22$ and $\kappa_d = 0.13$. These values, as well as the relatively long time needed to reach a plateau suggest extensive recrossings at the transition state. Closer examination of the initial behavior (Figure 10, insert) reveals interesting structural differences in the correlation functions. ξ_a shows a brief plateau while ξ_d does not. This suggests that ξ_a is a more physically relevant reaction coordinate than ξ_d. This agrees with the above discussion since the two intermolecular distances that define ξ_a also define two hydrogen bond acceptors, methanol and acetonitrile, competing for the same donor. As ξ_a decreases, methanol becomes the dominant acceptor and the reactive event moves toward the product side. Conversely, in ξ_d the two hydrogen-bonding distances are relatively impartial to the

other's existence, as evidenced by the sharp peak at $\xi_d = 0$ Å in Figure 8 and the flat silica-acetonitrile hydrogen bonding probability curve in Figure 9b.

We conclude by discussing the orientation of the methanol molecule at various locations along the two different reaction coordinate. Far from the surface, methanol's approach to the silica surface is driven by diffusion through acetonitrile liquid in which no particular orientation is preferred. Methanol ultimately attains a very precise orientation when bonded to the silica surface. Of obvious interest is the molecular orientation of the methanol molecule between these two extremes, in particular at the transition states as defined by the histogram in Figure 8. Methanol O-CH_3 and O-H molecular vectors are used to describe the orientation of the molecule at the ξ_d and ξ_a transition states. Figure 11 shows the orientational distributions of these molecular vectors relative to a vector normal to and pointing away from the silica surface.

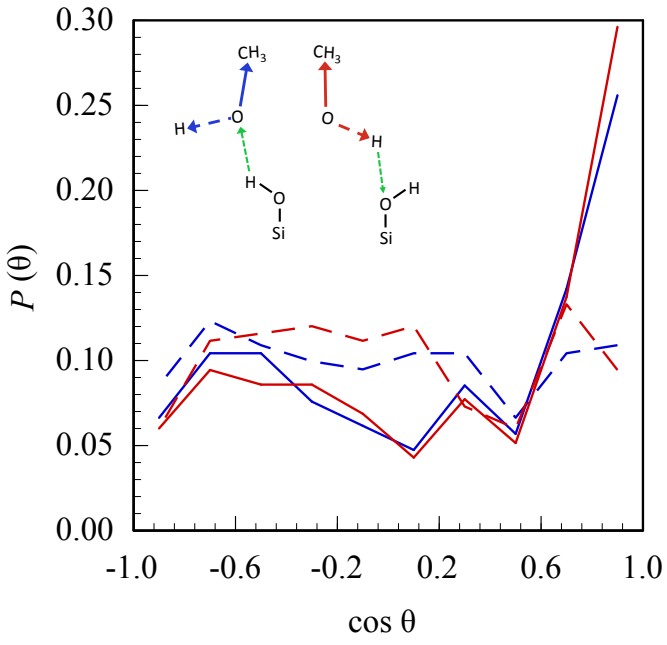

Figure 11. Orientational distributions of methanol molecular vectors relative to the surface normal at the reaction transition states ξ_d (red curves) and ξ_a (blue curves). Solid curves represent the methanol O-CH_3 vector and dashed curves represent the O-H vector.

In both ξ_d and ξ_a the O-CH_3 vector predominantly points away from the silica interface. We would anticipate that the nonpolar alkyl tail would "dislike" the hydrophilic surface and also that the methanol hydroxyl group should be in position to engage the silanol groups for hydrogen bonding to occur.

We may further describe methanol's orientation during this reactive event by considering the orientation preferred by methanol when hydrogen bonding with silica initially occurs. Figure 12 shows the orientational distributions of methanol molecular vectors, O-CH_3 and O-H, relative to a vector normal to and pointing away from the silica surface.

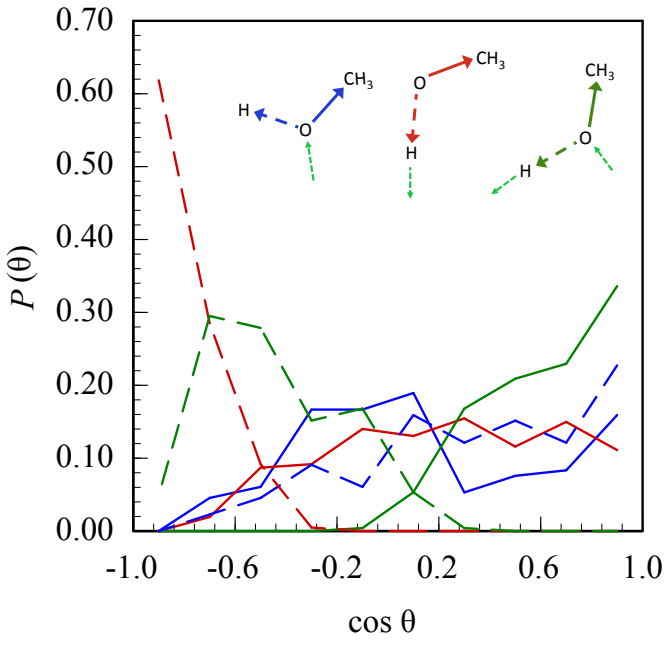

Figure 12. Orientational distributions of methanol molecular vectors at initial methanol-silica hydrogen bond formation where methanol participates as donor (red), acceptor (blue), or in two bonds as both donor and acceptor (green). Solid lines represent the O-CH_3 vector. Dashed lines represent the O-H vector.

We note that orientations for all bonding situations differ significantly from orientations at the transition state (Figure 11), where the O-CH_3 vectors predominantly point away from the silica surface and the O-H vectors lack a dominant orientation. When methanol's first hydrogen bonding interaction with silica is as a hydrogen bond donor, the O-H vector points toward the silica surface. When methanol first accepts a hydrogen bond from a silica site, the O-H vector is parallel to or pointing slightly away from the interface. When methanol is first bonded to two sites as both donor and acceptor, the molecule assumes the anticipated orientation, where the O-H vector points slightly toward the interface so that it may access silica oxygen and hydrogen atoms. The methyl tail, described by the O-CH_3 vector, points away from the polar surface.

IV. Conclusions

The molecular dynamics simulations described in this work present a detailed view of a mechanism by which a strongly hydrogen bonding solvent molecule (methanol) displaces a weakly hydrogen bonding solvent (acetonitrile) adsorbed at a hydrophilic (silica) surface. At equilibrium, for all the methanol/acetonitrile mixtures investigated here, methanol is much more strongly bonded to the silica surface as it is able to act as both hydrogen bond donor and acceptor to two neighboring silica sites, compared with acetonitrile which is able to act only as a hydrogen bond acceptor to one site. When a methanol molecule approaches the silica-acetonitrile system, it is able to effectively leverage its affinity to the silanol oxygen atom, a potential

hydrogen bond acceptor ignored by interfacial acetonitrile molecules. This displacement event may be visualized as a "bottle-opener" mechanism, where the methanol anchors itself to the silica surface by donating a hydrogen bond to the silica oxygen and subsequently rotates about its hydroxyl hydrogen atom, accepting a hydrogen bond from a neighboring silica hydrogen while dislodging the respective acetonitrile. The second possible mechanism is the initial approach of methanol, oriented to accept a hydrogen bond from the silica surface. In this configuration, methanol initially displaces acetonitrile and accepts a hydrogen bond from the silica surface and then donates a hydrogen bond to an adjacent silanol oxygen, ensuring stability at the silica surface.

Acknowledgments

This work has been supported by a grant from the National Science Foundation (CHE-1363076). We are grateful to Rob Walker and Eric Gobrogge for many useful conversations.

References

1. Guenther, U.; Smirnova, I.; Neubert, R. H. H. Hydrophilic silica aerogels as dermal drug delivery systems – Dithranol as a model drug. *Eur. J. Pharm. Biopharm.* **2008,** *69* (3), 935-942.

2. Smirnova, I.; Suttiruengwong, S.; Arlt, W. Aerogels: Tailor-made Carriers for Immediate and Prolonged Drug Release. *KONA* **2005,** *23*, 86-97.

3. Smirnova, I.; Suttiruengwong, S.; Arlt, W. Feasibility study of hydrophilic and hydrophobic silica aerogels as drug delivery systems. *J. Non-Cryst. Solids* **2004,** *350*, 54-60.

4. Ulker, Z.; Erkey, C. An emerging platform for drug delivery: Aerogel based systems. *J. Controlled Release* **2014,** *177*, 51-63.

5. Chemtob, S. M.; Rossman, G. R. Timescales and mechanisms of formation of amorphous silica coatings on fresh basalts at Kīlauea Volcano, Hawai'i. *JVGR* **2014,** *286*, 41-54.

6. Lis, D.; Backus, E. H. G.; Hunger, J.; Parekh, S. H.; Bonn, M. Liquid flow along a solid surface reversibly alters interfacial chemistry. *Science* **2014,** *344* (6188), 1138-1142.

7. Minakata, S.; Komatsu, M. Organic Reactions on Silica in Water. *Chem. Rev.* **2009,** *109* (2), 711-724.

8. Snyder, L. R.; Dolan, J. W.; Gant, J. R. Gradient elution in high-performance liquid chromatography : I. Theoretical basis for reversed-phase systems. *J. Chromatogr. A* **1979,** *165* (1), 3-30.

9. Dolan, J. W.; Gant, J. R.; Snyder, L. R. Gradient elution in high-performance liquid chromatography : II. Practical application to reversed-phase systems. *J. Chromatogr. A* **1979,** *165* (1), 31-58.

10. Horie, K.; Kamakura, T.; Ikegami, T.; Wakabayashi, M.; Kato, T.; Tanaka, N.; Ishihama, Y. Hydrophilic Interaction Chromatography Using a Meter-Scale Monolithic Silica Capillary Column for Proteomics LC-MS. *Anal. Chem.* **2014,** *86* (8), 3817-3824.

11. Melnikov, S. M.; Höltzel, A.; Seidel-Morgenstern, A.; Tallarek, U. Evaluation of Aqueous and Nonaqueous Binary Solvent Mixtures as Mobile Phase Alternatives to Water–Acetonitrile Mixtures for Hydrophilic Interaction Liquid Chromatography by Molecular Dynamics Simulations. *J. Phys. Chem. C* **2014,** *119* (1), 512-523.

12. Melnikov, S. M.; Höltzel, A.; Seidel-Morgenstern, A.; Tallarek, U. A Molecular Dynamics Study on the Partitioning Mechanism in Hydrophilic Interaction Chromatography. *Angew. Chem. Int. Ed.* **2012,** *51* (25), 6251-6254.

13. Collings, M. P.; Frankland, V. L.; Lasne, J.; Marchione, D.; Rosu-Finsen, A.; McCoustra, M. R. S. Probing model interstellar grain surfaces with small molecules. *MNRAS* **2015,** *449* (2), 1826-1833.

14. Roskosz, M.; Leroux, H. A Significant Amount of Crystalline Silica in Returned Cometary Samples: Bridging the Gap between Astrophysical and Meteoritical Observations. *Astrophys. J. Lett.* **2015,** *801* (1).

15. Rutigliano, M.; Gamallo, P.; Sayós, R.; Orlandini, S.; Cacciatore, M. A molecular dynamics simulation of hydrogen atoms collisions on an H-preadsorbed silica surface. *Plasma Sources Sci. Technol.* **2014,** *23* (4).

16. Eisenthal, K. B. Liquid Interfaces Probed by Second-Harmonic and Sum-Frequency Spectroscopy. *Chem. Rev.* **1996,** *96* (4), 1343-1360.

17. Shen, Y. R. Surfaces probed by nonlinear optics. *Surf. Sci.* **1994,** *299–300*, 551-562.

18. Shen, Y. R.; Ostroverkhov, V. Sum-frequency vibrational spectroscopy on water interfaces: polar orientation of water molecules at interfaces. *Chem. Rev.* **2006,** *106* (4), 1140-54.

19. Eftekhari-Bafrooei, A.; Borguet, E. Effect of surface charge on the vibrational dynamics of interfacial water. *J. Am. Chem. Soc.* **2009,** *131* (34), 12034-5.

20. Eftekhari-Bafrooei, A.; Borguet, E. Effect of hydrogen-bond strength on the vibrational relaxation of interfacial water. *J. Am. Chem. Soc.* **2010,** *132* (11), 3756-61.

21. Liu, W.; Zhang, L.; Shen, Y. R. Interfacial layer structure at alcohol/silica interfaces probed by sum-frequency vibrational spectroscopy. *Chem. Phys. Lett.* **2005,** *412* (1-3), 206-209.

22. Roy, D.; Liu, S.; Woods, B. L.; Siler, A. R.; Fourkas, J. T.; Weeks, J. D.; Walker, R. A. Nonpolar Adsorption at the Silica/Methanol Interface: Surface Mediated Polarity and Solvent

Density across a Strongly Associating Solid/Liquid Boundary. *J. Phys. Chem. C* **2013,** *117* (51), 27052-27061.

23. Siler, A. R.; Walker, R. A. Effects of Solvent Structure on Interfacial Polarity at Strongly Associating Silica/Alcohol Interfaces. *J. Phys. Chem. C* **2011,** *115* (19), 9637-9643.

24. Ding, F.; Hu, Z. H.; Zhong, Q.; Manfred, K.; Gattass, R. R.; Brindza, M. R.; Fourkas, J. T.; Walker, R. A.; Weeks, J. D. Interfacial Organization of Acetonitrile: Simulation and Experiment. *J. Phys. Chem. C* **2010,** *114* (41), 17651-17659.

25. Henry, M. C.; Wolf, L. K.; Messmer, M. C. In Situ Examination of the Structure of Model Reversed-Phase Chromatographic Interfaces by Sum-Frequency Generation Spectroscopy. *J. Phys. Chem. B* **2003,** *107* (12), 2765-2770.

26. Cimas, l.; Tielens, F.; Sulpizi, M.; Gaigeot, M.-P.; Costa, D. The amorphous silica-liquid water interface studied by ab initio molecular dynamics (AIMD): local organization in global disorder. *J. Phys.: Condens. Matter* **2014,** *26* (24).

27. Garofalini, S. H. Molecular dynamics computer simulations of silica surface structure and adsorption of water molecules. *J. Non-Cryst. Solids* **1990,** *120* (1-3), 1-12.

28. Lee, S. H.; Rossky, P. J. A comparison of the structure and dynamics of liquid water at hydrophobic and hydrophilic surfaces—a molecular dynamics simulation study. *J. Chem. Phys.* **1994,** *100* (4), 3334.

29. Skelton, A. A.; Fenter, P.; Kubicki, J. D.; Wesolowski, D. J.; Cummings, P. T. Simulations of the Quartz(101x1)/Water Interface: A Comparison of Classical Force Fields, Ab Initio Molecular Dynamics, and X-ray Reflectivity Experiments. *J. Phys. Chem. C* **2011,** *115* (5), 2076-2088.

30. Liu, S.; Fourkas, J. T. Orientational Time Correlation Functions for Vibrational Sum-Frequency Generation. 3. Methanol. *J. Phys. Chem. C* **2015,** *119* (10), 5542-5550.

31. Hu, Z.; Weeks, J. D. Acetonitrile on Silica Surfaces and at Its Liquid–Vapor Interface: Structural Correlations and Collective Dynamics. *J. Phys. Chem. C* **2010,** *114* (22), 10202-10211.

32. Norton, C. D.; Thompson, W. H. Reorientation Dynamics of Nanoconfined Acetonitrile: A Critical Examination of Two-State Models. *J. Phys. Chem. B* **2014,** *118* (28), 8227-8235.

33. Mountain, R. D. Molecular Dynamics Simulation of Water–Acetonitrile Mixtures in a Silica Slit. *J. Phys. Chem. C* **2013,** *117* (8), 3923-3929.

34. Gobrogge, E. A.; Walker, R. A. Binary Solvent Organization at Silica/Liquid Interfaces: Preferential Ordering in Acetonitrile–Methanol Mixtures. *J. Phys. Chem. Lett.* **2014,** *5* (15), 2688-2693.

35. Mountain, R. D. Microstructure and hydrogen bonding in water-acetonitrile mixtures. *J. Phys. Chem. B* **2010,** *114* (49), 16460-4.

36. Hemström, P.; Irgum, K. Hydrophilic interaction chromatography. *J. Sep. Sci.* **2006,** *29* (12), 1784-1821.

37. Cruz-Chu, E. R.; Aksimentiev, A.; Schulten, K. Water-silica force field for simulating nanodevices. *J. Phys. Chem. B* **2006,** *110* (43), 21497-508.

38. Leroch, S.; Wendland, M. Simulation of Forces between Humid Amorphous Silica Surfaces: A Comparison of Empirical Atomistic Force Fields. *J. Phys. Chem. C* **2012,** *116* (50), 26247-26261.

39. Benjamin, I.; Barbara, P. F.; Gertner, B. J.; Hynes, J. T. Nonequilibrium Free Energy Functions, Recombination Dynamics, and Vibrational Relaxation of I2- in Acetonitrile:

Molecular Dynamics of Charge Flow in the Electronically Adiabatic Limit. *J. Phys. Chem.* **1995,** *99* (19), 7557-7567.

40. Benjamin, I. Vibrational Spectrum of Water at the Liquid/Vapor Interface. *Phys. Rev. Lett.* **1994,** *73* (15), 2083-2086.

41. Norton, C. D.; Thompson, W. H. On the Diffusion of Acetonitrile in Nanoscale Amorphous Silica Pores. Understanding Anisotropy and the Effects of Hydrogen Bonding. *J. Phys. Chem. C* **2013,** *117* (37), 19107-19114.

42. See supplementary Figure S1.

43. Whitnell, R. M.; Wilson, K. R. Computational Molecular Dynamics of Chemical Reactions in Solution. In *Rev. Comput. Chem.*, Lipkowitz, K. B.; Boyd, D. B., Eds. John Wiley & Sons, Inc.: 1993; pp 67-148.

Table of Contents Figure